Behavioral/Systems/Cognitive

Modulation of the Innate Immune Response by NMDA Receptors Has Neuropathological Consequences

Isaias Glezer,[1,2] Hakima Zekki,[1] Cristoforo Scavone,[2] and Serge Rivest[1]

[1]Laboratory of Molecular Endocrinology, Centre Hospitalier Université Laval Research Center, and Department of Anatomy and Physiology, Laval University, Québec, Canada G1V 4G2, and [2]Department of Pharmacology, Institute of Biomedical Science, University of São Paulo, 05508-900 São Paulo, Brazil

The aim of this study was to determine whether glutamate receptors modulate the innate immune response in the brain of C3H/HeN and C3H/HeJ mice; the latter bear a loss of function in the toll-like receptor (TLR) 4 gene. Mice received an intrastriatal (IS) infusion of lipopolysaccharide (LPS), the exogenous ligand for *TLR4*, and were killed at several times thereafter. This treatment activated the transcription of a wide variety of genes involved in the control of the innate immune response. MK-801, an antagonist of NMDA glutamate receptor subtype, exacerbated the effects of the endotoxin in the brain of C3H/HeN mice but not in *TLR4*-deficient animals. The ipsilateral side of C3H/HeN mice exhibited stronger hybridization signals for the mRNA encoding TLR2, CD14, tumor necrosis factor-α, and inhibitory factor-$\kappa B\alpha$ at various times after the treatment combining MK-801 and LPS. This robust inflammatory response in the brain of C3H/HeN mice was not associated with any convincing signs of neurodegeneration or demyelination that was verified via numerous approaches and at time up to 2 weeks after injection. However, animals that received long-term IS infusion of LPS, together with MK-801, exhibited a significant increase in demyelination levels within the ipsilateral side. Our results demonstrate that binding of glutamate to its cognate NMDA receptor modulates LPS-induced innate immune reaction in a *TLR4*-dependent manner. This acute response may be crucial to eliminate bacterial cell wall components and minimizing tissue injury. However, sustained deregulation of proinflammatory signaling involving NMDA receptors leads to demyelination and is likely to be a mechanism participating in such pathological conditions.

Key words: **innate immune response; *in situ* hybridization histochemistry; inflammation; lipopolysaccharide; proinflammatory cytokines; microglia; macrophages; glutamate; demyelination**

Introduction

Mammalian toll-like receptors (TLRs) are receptors involved in the recognition of pathogen-associated molecular patterns (PAMPs) and also molecules responsible for mounting appropriate responses against microorganisms (Anderson, 2000). Lipopolysaccharide (LPS) is a well characterized inducer of innate immune response recognized by monocytes/macrophages through its binding to membrane CD14 receptors, which transfer LPS to TLR4 via myeloid differentiation protein 2 (Akira et al., 2001). A TLR4 missense mutation was identified in mouse strain C3H/HeJ (Poltorak et al., 1998), which is refractory to LPS, and deletion of TLR4 leads to a phenotype that lacks responses against LPS (Beutler, 2000). The stimulation of TLR4 triggers the activity of the nuclear factor κB (NF-κB) transduction pathway (Anderson, 2000). Nuclear translocation of NF-κB activates numerous proinflammatory genes that encode cytokines, chemokines, proteins of the complement system, enzymes, and other molecules essential for pathogen elimination by innate immune response (Ghosh et al., 1998).

Despite the beneficial role of microglial activation in immune-mediated host defense, microglial-derived proinflammatory molecules have been associated with neurodegenerative disorders. Activated microglia and astrocytes are found in the brain of Alzheimer's, Parkinson's, and Huntington's disease patients as well as individuals suffering of multiple sclerosis (MS) and amyotrophic lateral sclerosis (Pasinetti, 1998; Gonzales-Scarano and Baltuch, 1999; Nguyen et al., 2002). The serum and CSF of these patients also show elevated levels of immune molecules, such as interleukin (IL)-6, IL-1β, and tumor necrosis factor α (TNF-α) (Pasinetti, 1998; Gonzales-Scarano and Baltuch, 1999; Nguyen et al., 2002). IL-1β and TNF-α are secreted by activated parenchymal microglia and can be potent inducers of cell death in models of neurodegeneration (Pasinetti, 1998; Gonzales-Scarano and Baltuch, 1999; Nguyen et al., 2002).

Glutamate is the major excitatory neurotransmitter in the CNS, and the NMDA subtype of glutamate ionotropic receptors has been implicated in neurodegenerative diseases (Beal, 1995; Simonian and Coyle, 1996). NMDA antagonists attenuate the neuronal cell death induced by many brain insults, making

Received Aug. 29, 2003; revised Oct. 1, 2003; accepted Oct. 7, 2003.

This work was supported by the Canadian Institutes of Health Research [CIHR; the former Medical Research Council of Canada (MRCC)]. S.R. is an MRCC Scientist and holds a Canadian Research Chair in Neuroimmunology. I.G. is supported by grants from Conselho Nacional de Desenvolvimento Científico e Tecnológico (CNPq) (200842/01-3), Fundação de Amparo à Pesquisa do Estado de São Paulo (00/10679-0), and CIHR. H.Z. is supported by a studentship from the K. M. Hunter/CIHR, and C.S. is a research fellow of CNPq. We thank Dr. A. Israel (Institut Pasteur, Paris, France) for the mouse I$\kappa B\alpha$ cDNA, Dr. D. Radzioch (McGill University, Montréal, Canada) for the plasmid containing the mouse TNF-α cDNA, and Dr. K. Pahan (University of Nebraska, Lincoln, NE) for the mouse IL-12p40 cDNA.

Correspondence should be addressed to Dr. Serge Rivest, Laboratory of Molecular Endocrinology, Centre Hospitalier Université Laval Research Center, and Department of Anatomy and Physiology, Laval University, 2705 Boulevard Laurier, Québec, Canada G1V 4G2. E-mail: Serge.Rivest@crchul.ulaval.ca.

 0270-6474/03/2311094-10$15.00/0

NMDA receptor (NMDAR) blockade an attractive approach to prevent neuronal cell death (Beal, 1995). An interplay between glutamatergic transmission and glial response seems to occur because glutamate receptors are localized in glial cells, activated microglia releases molecules that signalize through NMDARs, and glutamate stimulates microglia to release TNF-α (Piani et al., 1992; Noda et al., 1999, 2000; Bezzi and Volterra, 2001; Schipke et al., 2001). Thus, glutamate seems to be a good candidate for mediating the cellular communication between neurons and microglia in both physiological and pathological states. Glutamatergic modulation of microglial cells has important consequences, because these cells are sensitive to minor changes in the microenvironment and they are the major effectors of the cerebral innate immune response that may lead to production of both neurotrophic and neurotoxic molecules (Heese et al., 1998; Stoll and Jander, 1999; Herx et al., 2000; Nguyen et al., 2002).

The aim of this study was, therefore, to determine whether the NMDAR antagonist MK-801 has the ability to alter the inflammatory response in the brain of C3H/HeN and C3H/HeJ mice in response to an intracerebral bolus of the endotoxin LPS. We also investigated the potential consequences of such response in the cerebral tissue via different approaches.

Materials and Methods

Animals

Adult male C3H/HeN mice (body weight, 25–29 gm; Charles River Canada, St. Constant, Québec, Canada), C3H/HeJ mice (Jax Mice; Jackson Laboratory, Bar Harbor, ME), or Sprague Dawley rats (body weight, ~250 gm; Charles River Canada) were acclimated to standard laboratory conditions (14/10 hr light/dark cycle; lights on at 6:00 A.M. and off at 8:00 P.M.) with *ad libitum* access to rodent chow and water. Animal breeding and experiments were conducted according to Canadian Council on Animal Care guidelines, as administered by the Laval University Animal Care Committee.

Experimental protocols

Acute intraparenchymal injections. Mice receiving intrastriatal (IS) injections were anesthetized with an intraperitoneal injection of avertin (2,2,2 tribromoethanol; Sigma-Aldrich, St. Louis, MO) and placed in a stereotaxic apparatus (David Kopf Instruments, Tujunga, CA). The right caudate putamen was reached using a small cannula (33 gauge) at the coordinates 0.0 mm anteroposterior, −2.0 mm lateral, and −3.0 mm dorsoventral according to a mouse brain atlas (Paxinos and Franklin, 2001). The animals received an infusion of either sterile pyrogen-free saline (1 μl), LPS (0.5 μg; from *Eschericia coli*; serotype O55:B5; Sigma L2880), a mixture of LPS (0.5 μg) and MK-801 maleate (1 μg; Sigma), or MK-801 (1 μg) over 2 min by means of a microinjection pump (model A-99; Razel Scientific Instruments, Stanford, CT). Three or four mice were used per group for each time point, for a total number of 96 mice for this experiment.

At different time points, after intraparenchymal injections (6, 24, and 72 hr and 2 weeks), animals were deeply anesthetized via an intraperitoneal injection of a mixture of ketamine hydrochloride and xylazine and then rapidly perfused transcardially with 0.9% saline, followed by 4% paraformaldehyde in 0.1 M borax buffer, pH 9.5, at 4°C. Brains were removed rapidly from the skulls, postfixed for 2–4 d, and then placed in a solution containing 10% sucrose diluted in 4% paraformaldehyde–borax buffer overnight at 4°C. The frozen brains were mounted on a microtome (Reichert-Jung; Cambridge Instruments Company, Deerfield, IL) and cut into 20 μm coronal sections from the olfactory bulb to the end of the medulla. The slices were collected in cold cryoprotectant solution (0.05 M sodium phosphate buffer, pH 7.3, 30% ethylene glycol, and 20% glycerol) and stored at −20°C.

Long-term intraparenchymal infusions. A chronic indwelling cannula was implanted as described previously (Nadeau and Rivest, 2003). Adult male rats were anesthetized with an intraperitoneal injection of a mixture (1 ml/kg body weight) of ketamine hydrochloride (91 mg/kg) and xylazine (9 mg/kg), and the site of injection was reached stereotaxically (David Kopf Instruments). With the incisor bar placed at 3.3 mm below the intraneural line (horizontal zero), the coordinates from bregma for the guide cannula (22 gauge; C313G; Plastic One, Roanoke, VA) were 0.0 mm anteroposterior, −3.0 mm lateral, and −2.8 mm dorsoventral, according to brain atlas (Paxinos and Watson, 1998). The guide cannula was secured with screws and cranioplastic cement [cranioplastic powder (Plastic One); Dentsply repair material (Dentsply International, York, PA)]. The rats were then housed individually for a 10 d recuperation period. During the first 3 d after the surgery, rats received once daily a subcutaneous injection of 8 ml of Ringer's lactate (Abbott Laboratories, Saint-Laurent, Canada) and 50 μl of ketoprofen (Rhône Mérieux Canada, Victoriaville, Canada). After the recovery period, a mini-osmotic pump (Alzet model 2004; Durect Corporation, Cupertino, CA), connected to an internal cannula (28 gauge; 14 mm long from the pedestal; C313I; Plastic One) with Intramedic polyethylene tubing (PE-50; inner diameter, 0.58 mm; outer diameter, 0.965 mm; Dow Corning, Midland, MI), was implanted subcutaneously in the interscapular region. The internal cannula was connected to the guide cannula, reaching the dorsoventral coordinate at −5.0 mm. The pumps (lot 10047-02; pumping rate, 0.29 μl/hr) were filled with vehicle solution (sterile saline), LPS (0.0718 μg/μl; yielding 0.5 μg/d), a mixture of LPS and MK-801 (LPS, 0.0718 μg/μl; MK-801, 0.1437 μg/μl; yielding 1 μg/d), or MK-801 (0.1437 μg/μl) and incubated at 37°C in sterile saline solution 48 hr before the implantation *in vivo*. The animals were killed 72 hr after implantation of the mini-osmotic pumps. Three or five rats per group were used for the intraparenchymal infusion of saline ($n = 3$), LPS ($n = 5$), LPS plus MK-801 ($n = 5$), or MK-801 ($n = 3$). Brain preparation was performed as described above, except for the coronal sections that were cut at 30 μm thickness.

cRNA probes and in situ *hybridization*

Plasmids were linearized, and the sense and antisense riboprobes were synthesized as described in Table 1. Radioactive cRNA copies were synthesized by incubation of 250 ng of linearized plasmid in 6 mM $MgCl_2$, 40 mM Tris, pH 7.9, 2 mM spermidine, 10 mM NaCl, 10 mM DTT, 0.2 mM ATP/GTP/CTP, 100 μCi of α -^{35}S-UTP (catalog number NEG 039H; DuPont-NEN, Boston, ME), 20 U of RNAsin (Promega, Madison, WI), and 10 U of T7, SP6, or T3 RNA polymerase for 60 min at 37°C (Table 1). Unincorporated nucleotides were removed using the ammonium acetate precipitation method; 100 μl of DNase solution (1 μl DNase, 5 μl of 5 mg/ml tRNA, and 94 μl of 10 mM Tris/10 mM $MgCl_2$) was added, and, 10 min later, a phenol-chloroform extraction was performed. The cRNA was precipitated with 80 μl of 5 M ammonium acetate and 500 μl of 100% ethanol for 20 min on dry ice. The pellet was dried and ressuspended in 50 μl of 10 mM Tris/1 mM EDTA. A concentration of 10^7 cpm probe was mixed into 1 ml of hybridization solution (500 μl formamide, 60 μl of 5 M NaCl, 10 μl of 1 M Tris, pH 8.0, 2 μl of 0.5 M EDTA, pH 8.0, 50 μl of 20× Dehart's solution, 200 μl of 50% dextran sulfate, 50 μl of 10 mg/ml tRNA, 10 μl of 1 M DTT, and 118 μl of DEPC water minus volume of probe used). This solution was mixed and heated for 10 min at 65°C before being spotted on slides.

Hybridization histochemical localization of TLR2, inhibitory factor κBα (IκBα), TNF-α, cluster of differentiation 14 (CD14), inducible nitric oxide synthase (iNOS), IL-12 p40, interferon (IFN)-γ, and NMDAR1 mRNA was performed on every 12th section of the entire rostrocaudal extent of each brain, as described previously (Laflamme et al., 1999). The sections were exposed at 4°C to x-ray films (Biomax; Kodak, Rochester, NY) for 1–3 d. The slides were thereafter defatted in xylene, dipped in NTB-2 nuclear emulsion (diluted 1:1 with distilled water; Kodak), exposed for 15 d (iNOS, IL-12, p40, and IFN-γ transcripts), 13 d (TLR2 and CD14 transcripts), 10 d (TNF-α), 7 d (IκBα transcript), or 4 d (NMDAR1 transcript). The slides were then developed in D19 developer (Kodak) for 3.5 min at 14–16°C, washed for 15 sec in water, and fixed in rapid fixer (Kodak) for 5 min. Tissues were thereafter rinsed in running distilled water for 1 hr, counterstained with thionin (0.25%), dehydrated through graded concentrations of alcohol, cleared in xylene, and coverslipped with distrene plasticizer xylene (DPX) mounting media (Electron Microscopy Science, Washington, PA).

Table 1. Plasmids and enzymes used for the synthesis of the cRNA probes

Plasmid	Vector	Length (bp)	Enzymes used for the sense probe	Enzymes used for the antisense probe	Source
Mouse TLR2	PCR-blunt II-topo	2278 (almost full)	*Spe*/T7	*Eco*RV/Sp6	Cloned by PCR[a]
Mouse IκBα	Bluescript SK II+	1114 (full)	*Hind*III/T3	*Bam*HI/T7	Dr. A. Israël (Institut Pasteur, Paris, France)
Mouse TNF-α	Bluescript SK II+	1300 (full + a 593 bp non-coding part)	*Bam*HI/T7	*Pst*I/T3	Subcloned from a PUc19 plasmid provided by Dr. M. Oliver (Laval University, Québec, Canada)
Mouse CD14	pRc/CMV (5.4 kb)	1500	*Hind*III/SP6	*Apa*I/T7	Dr. Regine Landmann (University Hospital, Basel, Switzerland)
Mouse iNOS	Bluescript SK II+	817	*Eco*RI/T7	*Kpn*I/T3	Subcloned from a Puc19 plasmid provided by Dr. M. Oliver
Mouse NMDAR1	pCMV-sport 6	3300	*Hind*II/Sp6	SalI/T7	American Type Culture Collection (Manassas, VA)
Mouse IL-12 p40	pCL-Neo (5.474 kb)	1050	*Not*I/T7	*Xho*I/T3	Dr. K. Pahan (Nebraska Medical Center University, Lincoln, NE)
Mouse IFN-γ	pGEMEX	550	*Eco*RI/SP6	*Hind*III/T3	Dr. I. Campbell (The Scripps Research Institute, La Jolla, CA)

[a] The DNA fragment of 2.278 kb corresponding to the almost complete coding sequence (2.355 kb) of the reported mouse TLR2 mRNA (nucleotides 307–2661; Genbank accession number AF185284) was amplified by PCR from a cDNA macrophage B10R cell line library using a pair of 23 bp oligonucleotide primers complementary to nucleotides 323–345 (5′-GGCTCTTCTGGATCTTGGTGGCC-3′) and 2579–2601 (5′-GGGCCACTCCAGGTAGGTCTTGG-3′).

Detection of neuronal cell death, demyelination, and histological analysis

The presence of neuronal cell death was investigated with the Fluoro-Jade B (FJB) method. Briefly, every 12th section of the whole rostrocaudal extent of each brain was mounted onto poly-L-lysine-coated slides, dried under vacuum for 2 hr, dehydrated through graded concentrations of alcohol (50, 70, and 100%; 1 min), rehydrated through graded concentrations of alcohol (100, 70, and 50%; 1 min), and rinsed for 1 min in distilled water. Then, the sections were dipped and shacked in potassium permanganate solution (0.06%) for 10 min and rinsed for 1 min in distilled water. Slides were next dipped and shacked into a solution containing a mixture of 0.0004% FJB (Histochem, Jefferson, AR) plus 0.1% acetic acid (Sigma-Aldrich) plus 0.0002% 4′,6′-diamidino-2-phenylindole (Molecular Probes, Eugene, OR) for 20 min. The slides were thereafter rinsed three times in distilled water (1 min each), dried, dipped in xylene three times (2 min each), and coverslipped with DPX.

Demyelination was determined via Luxol Fast Blue (LFB) staining. The brain sections mounted onto poly-L-lysine-coated slides were dehydrated through graded concentrations of alcohol (50, 70, and 95%; 1 min each) and incubated at 60°C for 6 hr in LFB solution [1% Solvent Blue 38 (Sigma) in 95% ethanol and 0.5% acetic acid]. The sections were then rinsed in 95% ethanol (1 min), 0.05% lithium carbonate (1–5 min; Sigma), and 70% alcohol (two dips). Thereafter, the slides were stained in 1% eosine Y solution (EM Diagnostic System, Gibbstown, NJ) for 30 sec, rinsed in water, incubated in 0.25% cresyl violet (Sigma) for 30 sec, rinsed in water, dehydrated through graded concentrations of alcohol (50, 70, 95, and 100%; 1 min each), cleared in xylene for 1 min (two times), and coverslipped with DPX.

Nissl stain was used as a general index of cellular morphology that may be altered in response to the different treatments.

Quantitative analysis

Quantitative analyses were performed as described previously (Nadeau and Rivest, 2003). Hybridization signals were quantified on x-ray films (Biomax). Briefly, transmittance values (optical density) of the hybridization signal were measured under a Northern Light Desktop Illuminator (Imaging Research) using a Sony Camera Video System attached to a Micro-Nikkor 55 mm-Vivitar extension tube set coupled with a computer and NIH Image software version 1.59/ppc [written by W. Rasband (National Institutes of Health, Bethesda, MD) and available from the internet by anonymous ftp from http://rsb.info.nih.gov/nih-image/download.html]. OD values for each pixel were calculated using a known standard of intensity and distance measurements from a logarithmic specter adapted from Bioimage Visage 110s (Millipore, Ann Arbor, MI). The entire hemisphere ipsilateral to the injection site was digitized and subjected to densitometric analysis, yielding measurements of mean density per area. The OD of each hemisphere was then corrected for the average background signal by subtracting the OD of area without positive signal located in the contralateral side. Four different brain sections at the level of caudate putamen were used for each animal.

The dorsal basal ganglia and hippocampus were selected for the semiquantification of NMDAR1 mRNA. These structures exhibited high constitutive NMDAR1 expression levels and strong transcriptional activation of immune-related genes in response to intracerebral LPS/MK-801 administration. Measurements were performed in 10 C3H/HeN and 10 C3H/HeJ mice, and data are reported as mean OD values (±SEM).

Demyelination was evaluated on digitalized LFB-stained sections within the corpus callosum and caudoputamen as described previously (Nadeau and Rivest, 2003). The rationale to measure LFB staining (index of myelinated fibers) in these regions is based on the pattern of the inflammatory wave that diffused across the dorsal basal ganglia and corpus collosum in response to cerebral infusions. Briefly, OD of corpus callosum and caudato putamen was measured using the NIH Image software, and values of the contralateral side were subtracted from those of the ipsilateral side of four different rostrocaudal levels and expressed as absolute values (mean ± SEM).

The statistical analysis was performed by a one- or two-way ANOVA, followed by a Bonferroni/Dunn test procedure as *post hoc* comparisons or Student's *t* test for NMDAR1 subunit mRNA levels.

Results

LPS-induced expression of TLR2 and CD14 is modulated by MK-801 in a TLR4-dependent manner

Figure 1 depicts representative hybridization signals in the brain of mice treated with saline, LPS, LPS/MK-801, or MK-801 alone. As expected, implantation of the cannula and the stress of infusion caused a low expression of TLR2 mRNA. Such a localized pattern of positive TLR2-expressing cells was found in the brain of both saline- and MK-801-infused mice (Fig. 1). This low signal contrasts with the intense and widespread transcriptional activation of TLR2 ipsilateral to the side of LPS infusion (Fig. 1*Ab*, LPS). MK-801 exacerbated the effects of endotoxin injected directly within the basal ganglia. At 24 hr, the signal was more intense in the brain of mice treated with the NMDAR antagonist and endotoxin (Fig. 1*Ac*). Semiquantitative analyses performed on x-ray films revealed a significant difference between the LPS- and LPS/MK-801-treated groups (Fig. 1*C*).

This amplification by MK-801 was essentially abolished in C3H/HeJ mice, because these mice were much less sensitive to either LPS alone or combined with the NMDAR antagonist (Fig. 1*B*). It is interesting to note that despite the lack of functional TLR4, a single intracerebral bolus of LPS was able to increase TLR2 expression in regions ipsilateral to the injection site. However, the signal was, to a great extent, lower in C3H/HeJ mice than in their wild-type controls, and MK-801 remained without significant effect in TLR4-mutant mice (Fig. 1*B*,*C*). These data indicate that the ability of glutamate and NMDARs to modulate the innate immune response in the brain is dependent on the prior binding of LPS to its receptor TLR4.

The same phenomenon took place for the gene encoding CD14 (Fig. 2). The endotoxin caused a profound increase in the transcriptional activation of the gene encoding LPS receptor in

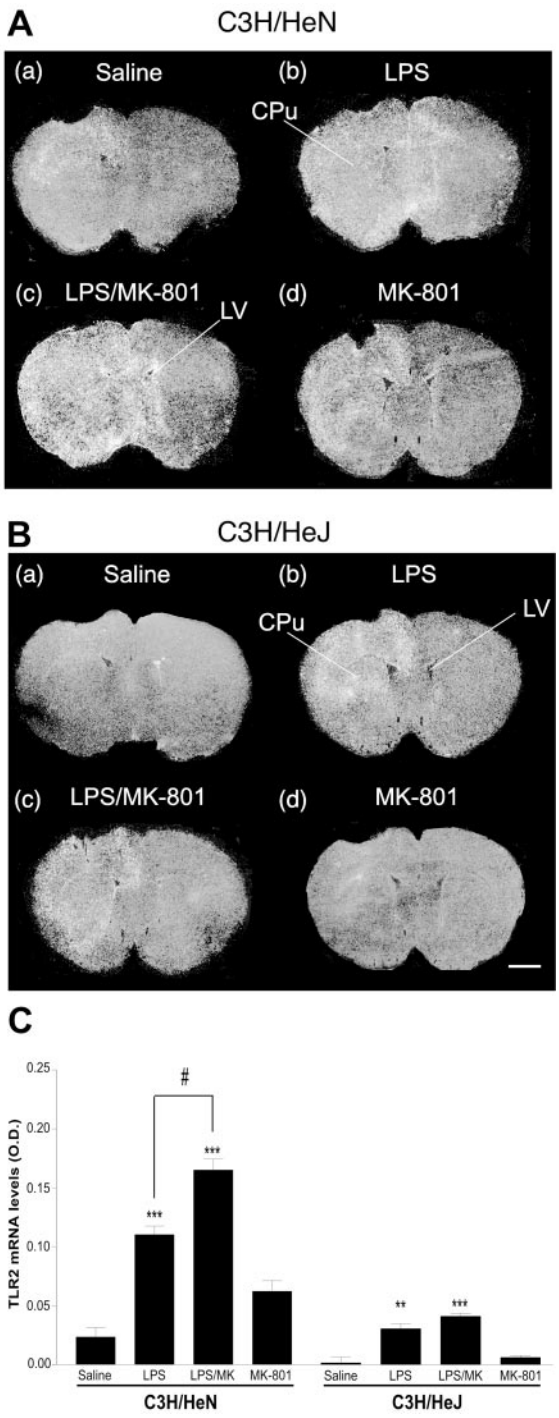

Figure 1. TLR2 mRNA expression in the brain of C3H/HeN and C3H/HeJ mice after an intraparenchymal bolus of saline, LPS, or the antagonist of the NMDAR MK-801. *A*, Representative hybridization signals in emulsion-dipped coronal sections (20 μm) taken from C3H/HeN mice that received only saline solution (*a*), LPS (*b*; 0.5 μg), a mixture containing LPS (0.5 μg) and MK-801 (*c*; 1 μg, LPS/MK-801), or MK-801 (*d*; 1 μg) in the dorsal basal ganglia. *B*, Emulsion-dipped coronal sections of C3H/HeJ mice, which bear a loss of function in the TLR4, killed 24 hr after a single bolus of saline solution (*a*), LPS (*b*), LPS combined with MK-801 (*c*), and MK-801 (*d*). *C*, Semiquantitative analysis of TLR2 mRNA levels (OD) in the ipsilateral side of C3H/HeN and C3H/HeJ mice 24 hr after the intracerebral insults. Please note the robust hybridization signal across the ipsilateral side of mice that received LPS combined with the antagonist of the NMDARs. Results represent means ± SEM of three to four mice per group. Statistical analysis was performed by using a two-way ANOVA, followed by a Bonferroni's multiple comparison test. **Significantly different ($p < 0.01$) from saline-injected group; ***significantly different ($p < 0.001$) from saline-injected group; #significantly different ($p < 0.05$). For more details, see Materials and Methods. CPu, Caudate putamen; LV, lateral ventricle. Scale bar, 1250 μm.

the ipsilateral side of mice killed 6 hr after the single intraparenchymal infusion. The cells lining the leptomeninges and few blood vessels exhibited a strong hybridization signal for CD14 transcript 6 hr after the cerebral injection with LPS alone or combined with MK-801 (Fig. 2*b*,*c*). As for TLR2, the expression wave across the brain parenchyma increased in intensity 24 hr after the treatment combining LPS with the antagonist of the NMDAR (Fig. 2*k*). This effect of MK-801 persisted up to 72 hr after injection, but the differences in the hybridization signal were not as marked as those found at 24 hr (Fig. 2*j*,*k*,*r s*). Once again, C3H/HeJ mice were relatively resistant to the treatments, but the endotoxin was capable of causing an increase in *CD14* gene expression in a localized area ipsilateral to the injection site at 6 hr (Fig. 2*f*,*g*). The signal largely decreased in the brain of these mice 24 hr after the intracerebral administration of the endotoxin that was combined or not with MK-801 (Fig. 2*n*,*o*). Seventy-two hours after the different treatments, very few positive CD14-expressing cells were found in the CNS of CH3/HeJ mice (Fig. 2*v*,*w*).

TLR4-dependent induction of proinflammatory signaling and gene transcription

The next series of assays evaluated whether expression of receptors involved in the innate immune response is associated with an increase in NF-κB signaling and transcriptional activation of genes encoding molecules involved in neurodegenerative disorders. The wave of TNF-α-expressing cells was characterized by strong signals at the edges of the inflammatory area restricted to the ipsilateral side 6 hr after LPS or LPS plus MK-801 infusions (Fig. 3*b*,*c*). At this time point, C3H/HeJ mice were relatively resistant to the endotoxin, although scattered positive TNF-α cells were detected in the infused region (Fig. 3*f*,*g*). Surprisingly, a robust hybridization signal was found in the brain of both mouse strains 24 hr after the single IS bolus of LPS (Fig. 3*j*,*k*,*n*,*o*). The message vanished quickly in the brain of C3H/HeJ mice (Fig. 3*v*,*w*), but remained positive and scattered across the injection site of C3H/HeN animals at 72 hr (Fig. 3*r*,*s*). The endotoxin is, therefore, able to trigger transcriptional activation of TNF-α in a very transient manner without a functional TLR4. Here, the effects of the antagonist of the NMDARs were not as convincing as for the other transcripts. However, TNF-α mRNA levels were, in general, higher in the CNS of most C3H/HeN mice treated with LPS and MK-801 and killed 6 hr afterward (Fig. 3*c*).

De novo induction of IκBα mRNA is a reliable index of NF-κB activity, and a strong hybridization was detected in the CNS of C3H/HeN mice (Fig. 4*A*). Indeed, IS infusion of LPS caused a diffuse pattern of positive cells across the brain parenchyma. The signal was already strong at 6 hr and remained positive up to 72 hr after LPS infusion (data not shown). The combined administration of LPS with the inhibitor of the NMDARs provoked a strong and widespread expression of IκBα mRNA in cells lining the ventricle ependyma, leptomeninges, blood vessels, and across the brain parenchyma ipsilateral to the injection site. The hybridization signal was clearly higher in the cerebral tissues of C3H/HeN mice treated with LPS and MK-801 than those of mice challenged only with the endotoxin and killed 6 hr afterward (Fig. 4*Ab*,*c*). It is interesting to note that mice killed 24 hr after the various treatments still exhibited a similar pattern of IκBα-expressing cells, but the message returned to a comparable level at 72 hr (data not shown). Although individual variations were observed among animals of that group, MK-801 was able to increase IκBα expression in response to LPS at 6 and 24 hr. IκBα mRNA levels were barely detectable in the brain of C3H/HeJ mice, which indicates

that exacerbation of the proinflammatory signaling by MK-801 depends on a functional TLR4.

Unlike the other transcripts, no positive signal was found for the gene encoding iNOS in the brain of C3H/HeJ mice in response to the endotoxin injected either alone or together with MK-801 (Fig. 4*B*). In C3H/HeN mice, the message significantly increased over the background level 6 hr after the intracerebral infusion of LPS alone or combined with MK-801 (Fig. 4*Bj*,*k*). At 24 hr, numerous clusters of iNOS-expressing cells were detected in the region infused with endotoxin, and the antagonist of the NMDARs failed to modulate the pattern of iNOS expression that was nonuniform and restricted to isolated clusters of positive cells (data not shown). The signal returned to background levels 72 hr after the IS infusion with the bacterial cell wall component combined or not with MK-801 (data not shown).

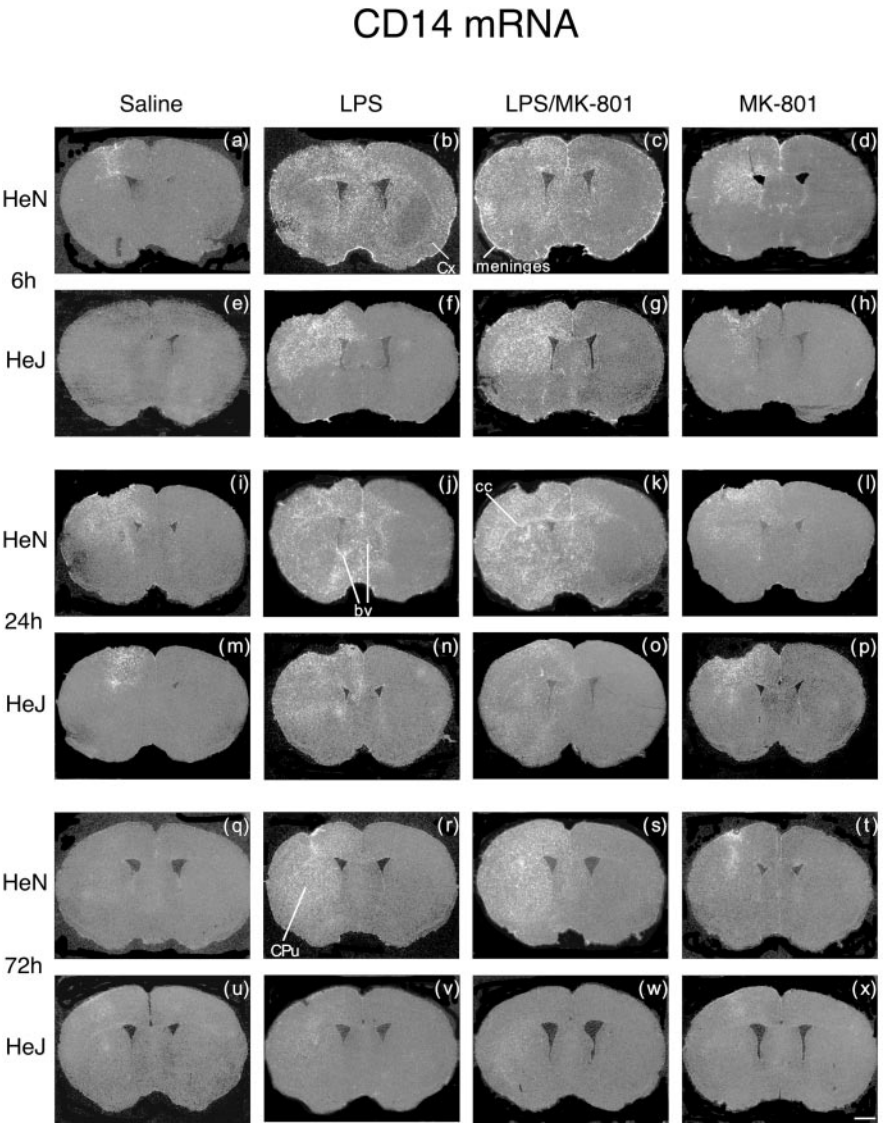

Figure 2. Time-related expression of CD14 mRNA in the brain of C3H/HeN and C3H/HeJ mice after a single intraparenchymal bolus of LPS and MK-801. These dark-field photomicrographs were taken from coronal sections hybridized with radioactive CD14 cRNA probe and dipped into nuclear emulsion milk. These images are representative examples of the expression pattern of CD14 transcript 6 hr (*a–h*), 24 hr (*i–p*), and 72 hr (*q–x*) after the infusion with saline, LPS, LPS plus MK-801, or MK-801 alone. Please note the robust signal in the area ipsilateral to the injection site of C3H/HeN mice challenged with LPS and MK-801. Although this effect was impaired in HeJ mice, the endotoxin was still capable of causing a significant increase in CD14 transcription in the brain of this strain (*f*, *g*). bv, Blood vessels; cc, corpus callosum; CPu, caudate putamen; Cx, cortex. Scale bar, 1000 μm.

NMDAR1 subunit expression in the brain of C3H/HeN and C3H/HeJ mice

To verify whether the NMDA antagonist failed to modulate LPS-induced immune response in C3H/HeJ mice because of a major difference in receptor expression, NMDAR1 subunit mRNA was measured via *in situ* hybridization histochemistry. As shown in Figure 5, the pattern and intensity of NMDAR1 gene expression were similar in the brain of both mouse strains. The distribution of the gene encoding this critical NMDAR was also similar to that already described in other studies (Laurie and Seeburg, 1994). Semiquantitative analyses were performed in caudate putamen and hippocampus because of the high expression levels and well-defined pattern of the receptor transcript in these structures. C3H/HeN and C3H/HeJ mice exhibited similar NMDAR1 mRNA levels in different regions of the brain (Fig. 5*C*).

Integrity of the neuronal elements

The consequences of altering the inflammatory response by MK-801 and TLR4 on the cerebral tissue were determined via two different approaches. FJB is a polyanionic fluorescein derivative that has been shown to be a sensitive and reliable marker for histochemical localization of neuronal degeneration (Schmued et al., 1997). Brain sections of animals with bilateral adrenalectomy were used as positive control, because a subpopulation of cells within the dentate gyrus granular layer are known to undergo neuronal cell death under this treatment. These neurons displayed strong and selective fluorescent FJB signals in the sections of a rat killed 6 d after being adrenalectomized (Fig. 6*Aa*). Such positive cells were never observed in the brain of LPS- or LPS plus MK-801-treated C3H/HeN mice 24 or 72 hr after infusions (Fig. 6*Ab–g*), except for the neurons adjacent to the cannula track. FJB neurons along the tract were found in all animals, including those infused only with vehicle solutions (Fig. 6*Ab*). Few capillaries of LPS-treated mice contained small and scattered positive cells, which are likely to be infiltrating cells (Fig. 6*Ad–f*, insets). Neurons remained negative for the fluorochrome FJB up to 2 weeks after the different treatments in both C3H/HeN and C3H/HeJ mice.

Nissl stain was also used to evaluate the morphology and histological integrity of the cerebral tissues. Figure 6*B* shows examples of brain sections taken from saline-, LPS-, or LPS plus MK-801-infused mice, and no convincing changes were observed 72 hr after the different treatments (Fig. 6*Ba–c*). The sections remained intact, and ipsilateral sides were similar to the contralateral areas at 2 weeks after LPS infusion in both mouse strains (Fig. 6*Bd–f*).

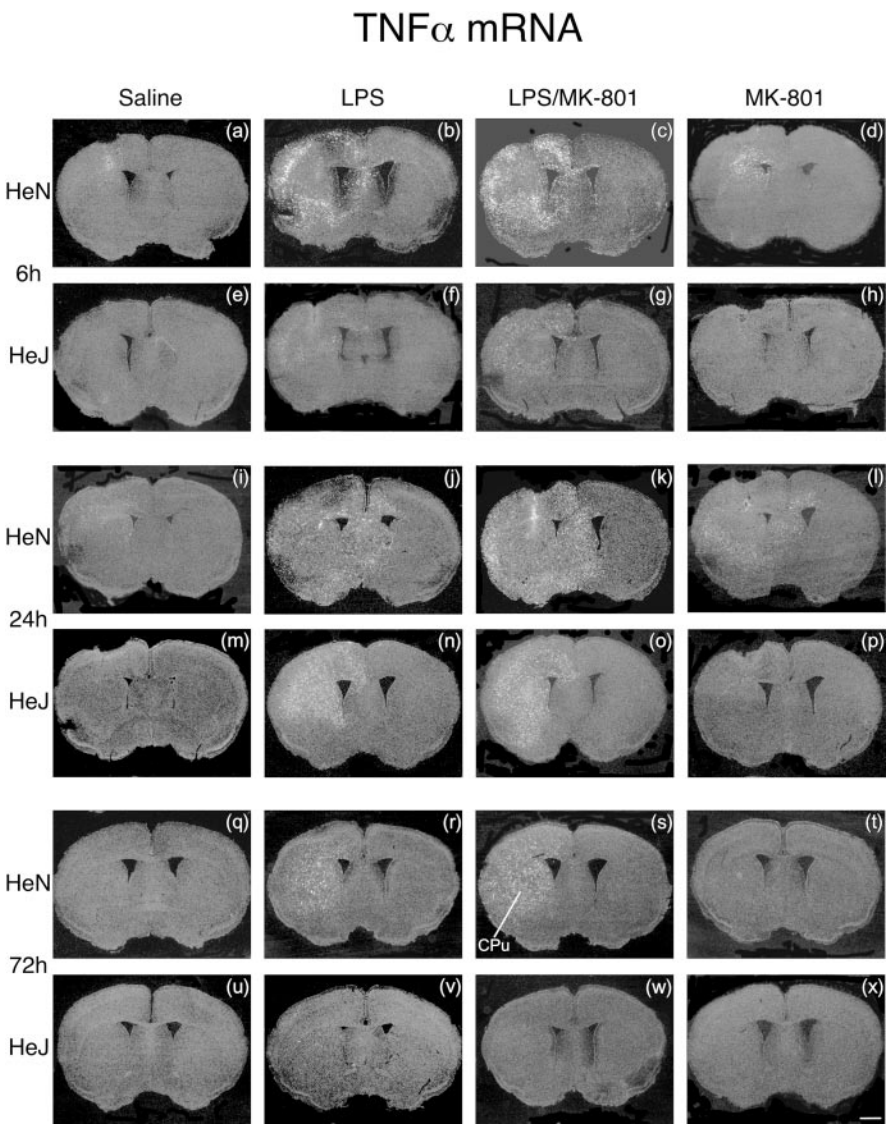

Figure 3. Expression wave of the proinflammatory cytokine TNF-α in response to intrastriatal infusion of LPS and MK-801. Representative nuclear emulsion dipped coronal sections depicting the effects of LPS and MK-801 on *TNF*α gene expression in C3H/HeN and C3H/HeJ mouse brains at 6 hr (*a–h*), 24 hr (*i–p*), and 72 hr (*q–x*) after injections. Please note the rapid expression of the gene encoding the cytokine in the brain of C3H/HeN mice after coadministration of LPS and MK-801. The endotoxin also stimulated *TNF-*α gene expression in the CNS of C3H/HeJ mice, especially at 24 hr (*n*, *o*). CPu, Caudate putamen. Scale bar, 1000 μm.

Genes involved in the transfer from the innate to adaptive immunity

The gene encoding TLR2 was still expressed in the brains of C3H/HeN mice 2 weeks after the single bolus of LPS (Fig. 7*a*) but not in those of C3H/HeJ mice (Fig. 7*b*). Few positive and small scattered IκBα- and TNF-α-expressing cells were also found, but the cerebral tissues of all groups remained without detectable signal for both IL-12 and IFN-γ transcripts. Positive controls for these two genes were hybridized in the brains of mice infected with herpes simplex virus type 2, which causes a profound neurodegeneration associated with innate and adaptive immune responses (Boivin et al., 2002).

Brain damage caused by a long-term infusion

To verify the relevance of innate immune response modulated by glutamate to brain physiopathology, an experimental protocol was designed to expose the cerebral tissue to long-term stimulation. Figure 8 depicts LFB-stained sections from animals treated with saline, LPS, LPS combined with MK-801, or MK-801 alone during 72 hr. Animals that received combined treatment of LPS plus MK-801 exhibited a striking degree of demyelination compared with the other groups, which was confirmed by semiquantitative analysis of differential OD with the contralateral side (Fig. 8*A*,*B*). LPS infusion for a period of 3 d was also able to cause demyelination, but differential OD failed to reach statistical significance because of the high degree of variability among animals of this group (Fig. 8*A*,*B*). It is possible that variable diffusions throughout the brain parenchyma contribute to different degrees of demyelination between animals and dorsoventral–rostrocaudal levels. However, demyelination was clear in all animals that received the double treatment, which was not the case in the cerebral tissue of rats that were infused only with the endotoxin. Demyelination was apparently not associated with neuronal cell death, because no positive FJB neurons were found in the brain of chronically treated rats. This pattern of demyelination was never observed in the brain of C3H/HeN or C3H/HeJ mice that received an acute bolus with the different solutions (data not shown).

Discussion

Innate immune response is crucial for protecting the brain and maintaining its integrity against invading microorganisms. Characterization of TLRs highlighted the existence of receptors for recognizing specific PAMPs and mounting an organized response to eliminate pathogens. TLR4 is believed to be an essential receptor for proper response to LPS but not other PAMPs (Anderson, 2000). Unexpectedly, TLR4 seems to be a receptor involved in the responses of myeloid cells to Taxol and some heat shock proteins, implying that TLR4 can also be a detector of "danger signals" (Underhill and Ozinsky, 2002; Wallin et al., 2002). TLR4 mRNA is expressed at low levels in the brain under basal conditions, and downregulation takes place in response to LPS injected either systemically or centrally (Laflamme and Rivest, 2001; Nadeau and Rivest, 2002). TLR4 is also critical for mediating the proinflammatory signaling and gene transcription in response to an IS LPS injection, because induction of most genes evaluated in this study was clearly impaired in the cerebral tissue of C3H/HeJ mice.

Although C3H/HeJ mice were relatively insensitive to LPS, the endotoxin was still capable of triggering gene expression in the CNS of these mice. However, strong differences were observed in the time of induction and between the different transcripts. For example, TNF-α mRNA levels were strong 24 hr after the IS LPS infusion, but the signal essentially vanished at 72 hr in the brains of these animals whereas it remained high in those of C3H/HeN mice. The ability of C3H/HeJ mice to exhibit a low, but signifi-

cant, response to LPS implies that signaling pathways, other than those mediated by TLR4, may take place in the brain. It is indeed possible that high concentrations of LPS within the injection site stimulate low affinity receptors expressed in a subpopulation of microglia/macrophages specifically within the CNS. It is also possible that induction of proinflammatory cytokines by cells lining the cannula track promotes expression of such low-affinity receptors and then increases signaling once the endotoxin cognates to these putative receptors. TLR4- and CD14-independent mechanisms have already been proposed for neutrophil recruitment and LPS clearance (Haziot et al., 2001).

In contrast to most genes analyzed here, *in situ* hybridization failed to detect any positive signal for iNOS in the cerebral tissue of C3H/HeJ mice challenged with the endotoxin combined with vehicle or MK-801. The gene encoding iNOS has been identified recently as one of a class of genes dependent of IFN-Iβ, which is produced by macrophages in response to different cell wall components (Toshchakov et al., 2002). It is, therefore, possible that other receptors mediate the effects of LPS in the cerebral tissue or endogenous released soluble molecules are responsible to trigger expression of genes, such as iNOS.

In this regard, innate immune response in the CNS is the result of a coordinated expression of cytokines and other inflammatory mediators in response to infection and insults. It remains, however, difficult to analyze the exact consequences of this response during pathological conditions. There is now compelling evidence of a bilateral talk between glia and neurons, and molecules involved in such interaction may play key roles in neurodegenerative processes. Glutamate is a putative mediator, because it is a major excitatory neurotransmitter and its metabolism and synaptic concentrations are regulated by astrocytes. Various glutamate receptor subtypes are expressed in astrocytes, oligodendrocytes, as well as in microglia (Noda et al., 2000; Bezzi and Volterra, 2001; Matute et al., 2001). Even more attractive is the fact that glutamatergic neurotoxicity has been implicated in many neurodegenerative diseases, especially at the level of NMDA receptor subtype, and molecules acting through NMDA are released by immune-stimulated macrophages and during neuroinflammatory diseases (Piani et al., 1992; Bezzi et al., 2001; Kaul et al., 2001).

The coadministration of LPS and noncompetitive antagonist MK-801 increased the expression levels of TLR2 mRNA and other inflammatory genes, which supports the concept that glutamatergic pathways can modulate immune reaction in the brain. It is interesting to note that MK-801 did not exacerbate the effects of LPS on all the genes assayed here, and the role of glutamate cannot be generalized to all the transcriptional processes that take place in response to an intracerebral bolus of LPS. However, the genes that were significantly modulated by the antagonist of the NMDARs were clearly dependent on the previous binding of LPS to its receptor TLR4. Although the impaired response to the endotoxin in C3H/HeJ mice may explain the failure of MK-801 to modulate the effects of LPS, inflammation is still induced in the brain of these animals. The ability of MK-801 to exacerbate the immune response to LPS should, therefore, be detectable with such mild microglial reactivity. However, this was not the case, and the interaction between the endotoxin and NMDARs was observed only in C3H/HeN mice, which indicates that TLR4 plays a critical role in this process. It is also possible that MK-801 acts only in presence of a robust immune reaction, such as in LPS-treated C3H/HeN mice. This led us to propose that a full response to LPS, which is TLR4 dependent, could be essential for the ability of NMDARs to modulate proinflammatory signaling and gene transcription.

MK-801 has been found recently to be toxic for microglial cells in culture, which underscores the existence of NMDARs in these cells (Hirayama and Kuriyama, 2001). Inhibition of NMDARs also has the ability to increase IFN-γ -induced expression of major histocompatiblity complex class II in microglia *in vivo* (McCluskey and Lampson, 2001). Taken together, these data indicate that NMDARs are novel players in the control of the innate immune system in the presence of cell wall components derived from Gram-negative bacteria.

Despite the robust inflammatory response and changes in the signal intensity by MK-801, no signs of neurodegeneration were

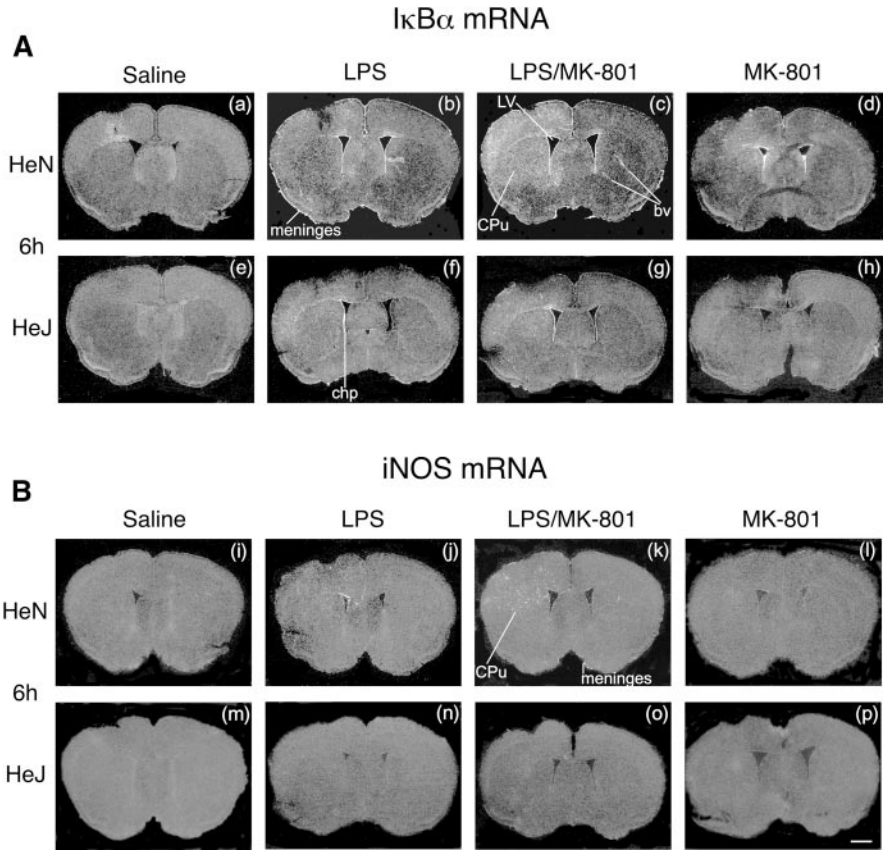

Figure 4. TLR4-dependent effects of MK-801 on LPS-induced *IκBα* and *iNOS* gene expression. *A*, Dark-field photomicrographs taken from coronal sections hybridized with radioactive IκBα cRNA probe and dipped into nuclear emulsion milk. These images are representative examples of the expression pattern of IκBα transcript (used here as an index of NF-κB activity) (*a–h*) 6 hr after the infusion with saline, LPS, LPS plus MK-801, or MK-801 alone. *B*, Positive signals for iNOS mRNA were only detected in C3H/HeN mice treated with LPS or LPS plus MK-801 (*j* and *k*, respectively) 6 hr after the infusion. The cerebral tissues of C3H/HeJ mice failed to show any positive signal for the mRNA encoding iNOS. bv, Blood vessels; cc, corpus callosum; chp, choroid plexus; CPu, caudate putamen; LV, lateral ventricle. Scale bar, 1000 μm.

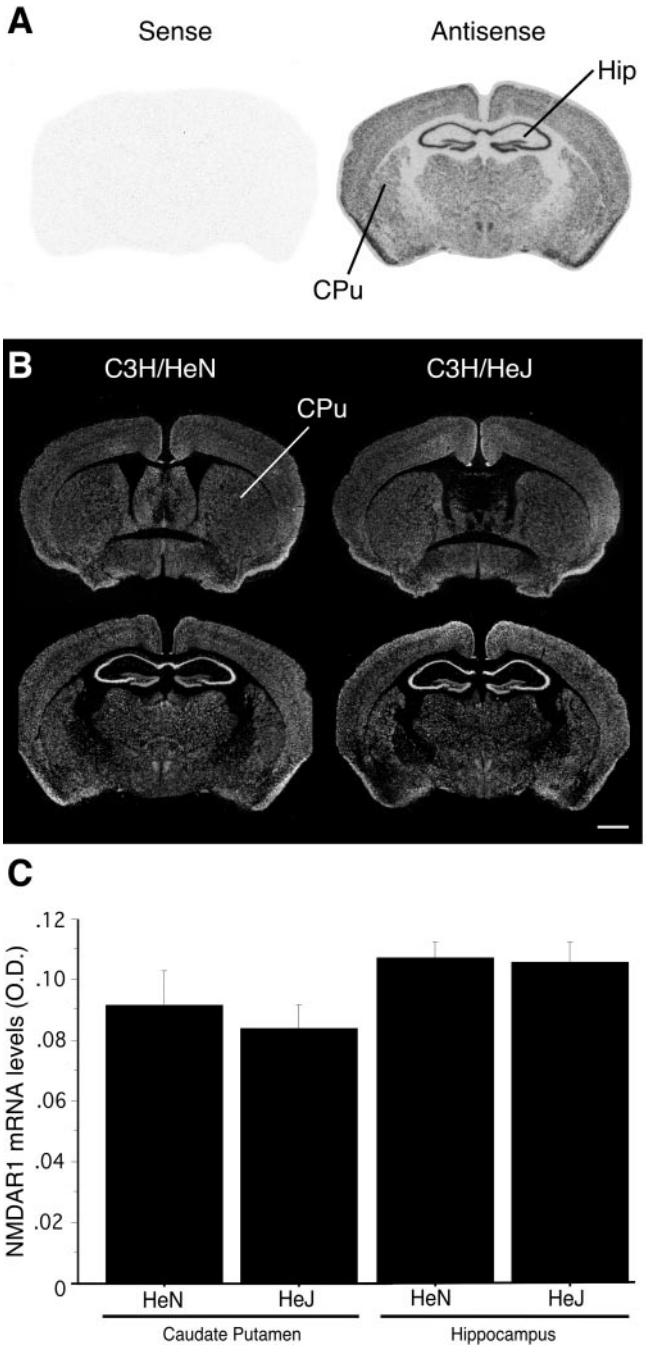

Figure 5. Expression of NMDAR1 subunit mRNA in the brain of C3H/HeN and C3H/HeJ mice. *A*, Representative signals in coronal sections hybridized with sense or antisense riboprobe and exposed to x-ray films (Biomax; Kodak). *B*, Dark-field photomicrographs taken from coronal sections hybridized with radioactive NMDAR1 cRNA probe and dipped into nuclear emulsion milk. Intensity and pattern of the hybridization signal were similar across the brains of C3H/HeN and C3H/HeJ mice. *C*, Semiquantitative analysis of relative NMDAR1 mRNA levels (OD) in the caudate putamen (CPu) and hippocampus (Hip) of C3H/HeN and C3H/HeJ mice. Scale bar, 1000 μm.

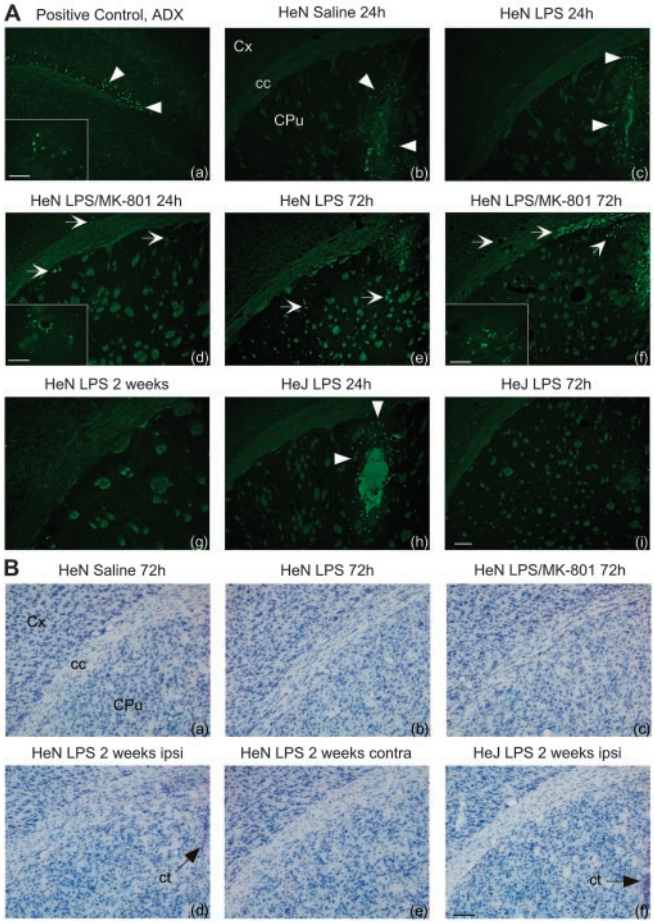

Figure 6. Neuronal integrity in the brain of C3H/HeN and C3H/HeJ mice after intrastriatal infusion of LPS and the antagonist of NMDARs. *A*, The fluorochrome FJB was used as a marker for histochemical localization of degenerative neurons. Degenerating neurons (positive control) were found in hippocampus of a rat killed 6 d after being adrenalectomized (*a*, inset). Such positive neurons were never observed in regions depicting the robust expression of the different transcripts, except along the needle track because of the mechanical injury (white arrowheads). Small non-neuronal cells (probably infiltrating cells) were also found in the CNS of C3H/HeN mice treated with LPS alone or combined with MK-801 (white arrows). *B*, Nissl-stained sections at the level of dorsal basal ganglia. Neuronal density and morphology were similar among all the groups included in this study. Black arrows point to the cannula track. Cx, Cortex; cc, corpus callosum; contra, contralateral side; CPu, caudate putamen; ipsi, ipsilateral side; ct, cannula track. Scale bars, 100 μm; insets, 50 μm.

observed via FJB and Nissl stain techniques. This was also the case in the brain of C3H/HeJ mice that exhibited impairment of the immune reaction after IS infusions with the different solutions. Although TLR2 mRNA signal was still positive 2 weeks after LPS infusion in C3H/HeN mice, the brain of these animals failed to show any signs of altered neuronal morphology and neurodegeneration. This is further supported by the negative signal for the cytokine IFN-γ and IL-12, which could be associated with an adaptive immune response linked to a chronic inflammatory process. The physiological relevance of the long-term expression of TLR2 in response to a single bolus of LPS still remains to be clarified.

In disagreement with this study and others (Szczepanik et al., 1996; Nadeau and Rivest, 2002) are the reports that provided evidence of LPS-induced neurotoxicity (Castano et al., 1998; Kim et al., 2000). Different techniques used for assaying neurodegeneration and regional neuronal susceptibility or regional density of microglial cells may explain the discrepancies between the studies. In the present case, microglial activation was robust and, because of the lack of convincing signs of neurodegeneration, we propose that acute innate immune response is not detrimental for the cerebral tissue. In contrast, uncontrolled immune response can have profound detrimental consequences for the cerebral elements (Nadeau and Rivest, 2003; Soulet and Rivest, 2003). Our results demonstrate that long-term infusion of LPS

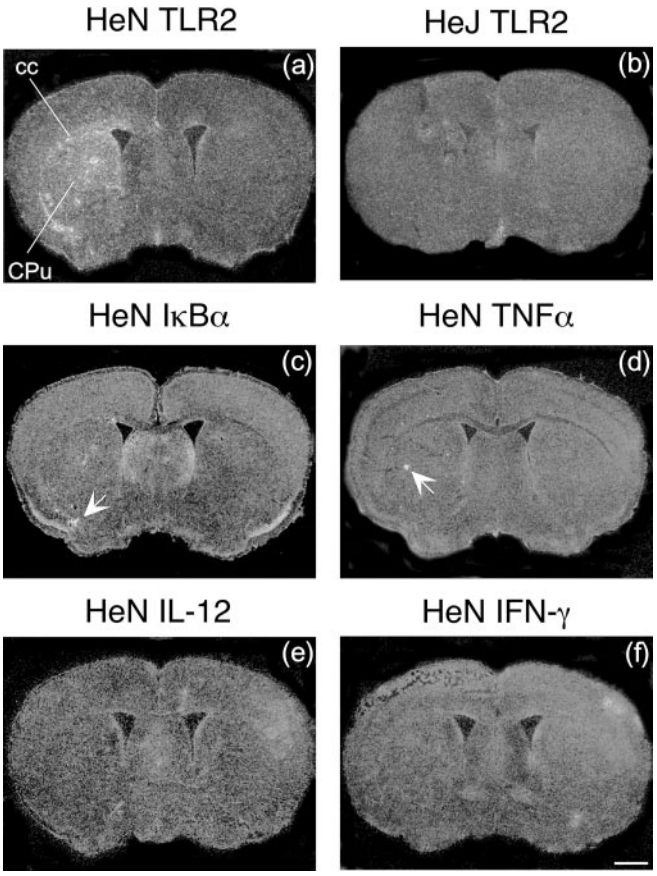

Figure 7. The innate immune response is not associated with a transfer to the adaptive immunity. Representative examples of nuclear emulsion-dipped coronal sections depicting expression of genes involved in the transfer from the innate to adaptive immune response 2 weeks after LPS injection in the dorsal striatum. TLR2 mRNA was still expressed in the ipsilateral side of C3H/HeN mice 14 d after a single bolus of LPS (*a*), whereas such signal was not present in the infused regions of C3H/HeJ mice (*b*). Few IκBα- and TNF-α-expressing cells were also found in the brain of C3H/HeN mice (*c*, *d*, white arrows). *In situ* hybridization failed to detect any positive signal for IL-12 and IFN-γ across the cerebral tissue of C3H/HeN mice (*e* and *f*, respectively). cc, Corpus callosum; CPu, caudate putamen. Scale bar, 1000 μm.

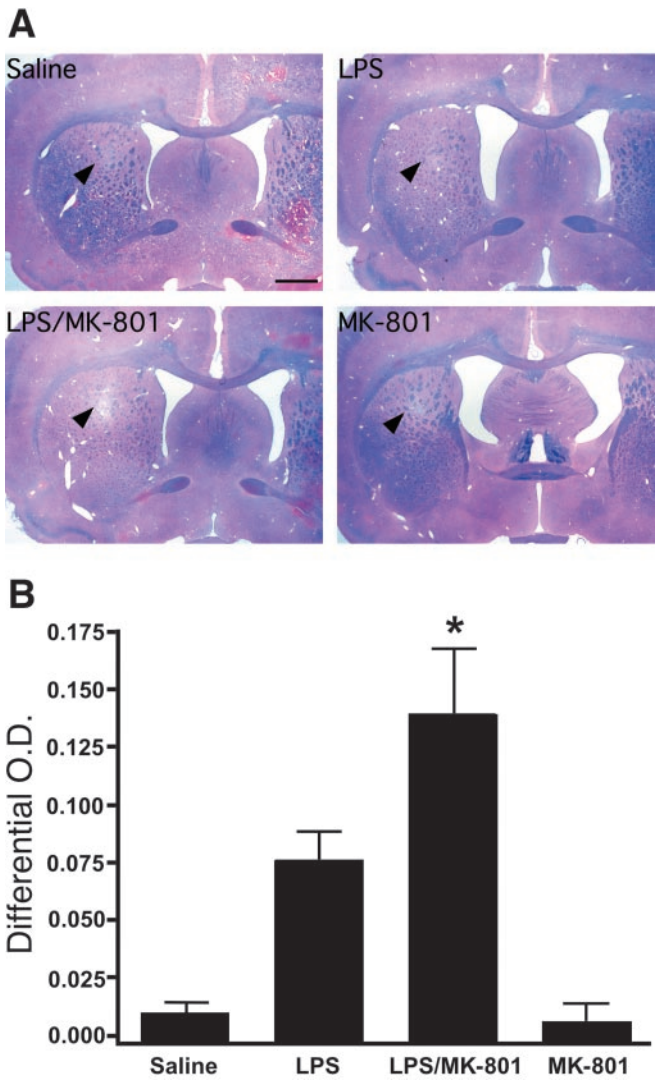

Figure 8. Demyelination in response to long-term infusion of the endotoxin LPS and NMDAR antagonist MK-801 in ipsilateral sides of adult male SD rats. *A*, Luxol Fast Blue-stained coronal sections from animals infused with saline, LPS (0.5 μg/d), LPS combined with MK-801 (1 μg/d), or MK-801 alone and killed 72 hr after implantation of mini-osmotic pumps. *B*, Differential OD measured in several rostrocaudal sections of each rat included in this experiment. Statistical analysis was performed by using a one-way ANOVA, followed by a Bonferroni's multiple comparison test.*Significantly different ($p < 0.01$) from the saline-injected group. For more details on image analysis, see Materials and Methods. Black arrowheads indicate the tip of the cannula. Scale bar, 1250 μm.

combined with an NMDAR antagonist is able to provoke demyelination, which is a critical component in neurodegenerative diseases such as Alzheimer's disease (de la Monte, 1989; Roher et al., 2002; Pak et al., 2003). These data, together with the fact that glutamate unbalance takes place in MS (Werner et al., 2001), indicate that deregulation of the immune response by NMDARs may have a determinant role in brain disorders, especially in demyelinating diseases.

In conclusion, TLR4 is crucial for MK-801 to modulate the innate immune reaction in response to intraparenchymal LPS bolus. The robust and transient inflammatory wave induced by the bacterial cell wall component and NMDAR antagonist was not associated with cell death in the CNS. In contrast, long-term exposure to the same treatment provokes demyelination. There is, therefore, a fine line between beneficial and detrimental properties of immune-related compounds in the brain, and NMDARs may play a determinant role in this equilibrium.

References

Akira S, Takeda K, Kaisho T (2001) Toll-like receptors: critical proteins linking innate and acquired immunity. Nat Immunol 2:675–680.

Anderson KV (2000) Toll signaling pathways in the innate immune response. Curr Opin Immunol 12:13–19.

Beal MF (1995) Aging, energy, and oxidative stress in neurodegenerative diseases. Ann Neurol 38:357–366.

Beutler B (2000) Tlr4: central component of the sole mammalian LPS sensor. Curr Opin Immunol 12:20–26.

Bezzi P, Volterra A (2001) A neuron-glia signalling network in the active brain. Curr Opin Neurobiol 11:387–394.

Bezzi P, Domercq M, Brambilla L, Galli R, Schols D, De Clercq E, Vescovi A, Bagetta G, Kollias G, Meldolesi J, Volterra A (2001) CXCR4-activated astrocyte glutamate release via TNFα: amplication by microglia triggers neurotoxicity. Nat Neurosci 4:702–710.

Boivin G, Coulombe Z, Rivest S (2002) Intranasal herpes simplex virus type 2 inoculation causes a profound thymidine kinase dependent cerebral inflammatory response in the mouse hindbrain. Eur J Neurosci 16:29–43.

Castano A, Herrera AJ, Cano J, Machado A (1998) Lipopolysaccharide intranigral injection induces inflammatory reaction and damage in nigrostriatal dopaminergic system. J Neurochem 70:1584–1592.

de la Monte SM (1989) Quantitation of cerebral atrophy in preclinical and end-stage Alzheimer's disease. Ann Neurol 25:450–459.

Ghosh S, May MJ, Kopp EB (1998) NF-κB and rel proteins: evolutionary conserved mediators of immune responses. Annu Rev Immunol 16:225–260.

Gonzales-Scarano F, Baltuch G (1999) Microglia as mediators of inflammatory and degenerative diseases. Annu Rev Neurosci 22:219–240.

Haziot A, Hijiya N, Gangloff SC, Silver J, Goyert SM (2001) Induction of a novel mechanism of accelerated bacterial clearance by lipopolysaccharide in CD14-deficient and Toll-like receptor 4-deficient mice. J Immunol 166:1075–1078.

Heese K, Fiebich BL, Bauer J, Otten U (1998) NF-kappaB modulates lipopolysaccharide-induced microglial nerve growth factor expression. Glia 22:401–407.

Herx LM, Rivest S, Yong VW (2000) Central nervous system-initiated inflammation and neurotrophism in trauma: IL-1 beta is required for the production of ciliary neurotrophic factor. J Immunol 165:2232–2239.

Hirayama M, Kuriyama M (2001) MK-801 is cytotoxic to microglia in vitro and its cytotoxicity is attenuated by glutamate, other excitotoxic agents and atropine. Possible presence of glutamate receptor and muscarinic receptor on microglia. Brain Res 897:204–206.

Kaul M, Garden GA, Lipton SA (2001) Pathways to neuronal injury and apoptosis in HIV-associated dementia. Nat Neurosci 410:988–994.

Kim WG, Mohney RP, Wilson B, Jeohn GH, Liu B, Hong JS (2000) Regional difference in susceptibility to lipopolysaccharide-induced neurotoxicity in the rat brain: role of microglia. J Neurosci 20:6309–6316.

Laflamme N, Rivest S (2001) Toll-like receptor 4: the missing link of the cerebral innate immune response triggered by circulating gram-negative bacterial cell wall components. FASEB J 15:155–163.

Laflamme N, Lacroix S, Rivest S (1999) An essential role of interleukin-1beta in mediating NF-kappaB activity and COX-2 transcription in cells of the blood–brain barrier in response to a systemic and localized inflammation but not during endotoxemia. J Neurosci 19:10923–10930.

Laurie DJ, Seeburg PH (1994) Regional and developmental heterogeneity in splicing of the rat brain NMDAR1 mRNA. J Neurosci 14:3180–3194.

Matute C, Alberdi E, Domercq M, Perez-Cerda F, Perez-Samartin A, Sanchez-Gomez M (2001) The link between excitotoxic oligodendroglial death and demyelinating diseases. Trends Neurosci 24:224–230.

McCluskey LP, Lampson LA (2001) Local immune regulation in the central nervous system by substance P vs. glutamate. J Neuroimmunol 116:136–146.

Nadeau S, Rivest S (2002) Endotoxemia prevents the cerebral inflammatory wave induced by intraparenchymal lipopolysaccharide injection: role of glucocorticoids and CD14. J Immunol 169:3370–3381.

Nadeau S, Rivest S (2003) Glucocorticoids play a fundamental role in protecting the brain during innate immune response. J Neurosci 23:5536–5544.

Nguyen MD, Julien JP, Rivest S (2002) Innate immunity: the missing link in neuroprotection and neurodegeneration? Nat Rev Neurosci 3:216–227.

Noda M, Nakanishi H, Akaike N (1999) Glutamate release from microglia via glutamate transporter is enhanced by amyloid-beta peptide. Neuroscience 92:1465–1474.

Noda M, Nakanishi H, Nabekura J, Akaike N (2000) AMPA-kainate subtypes of glutamate receptor in rat cerebral microglia. J Neurosci 20:251–258.

Pak K, Chan SL, Mattson MP (2003) Presenilin-1 mutation sensitizes oligodendrocytes to glutamate and amyloid toxicities, and exacerbates white matter damage and memory impairment in mice. Neuromol Med 3:53–64.

Pasinetti G (1998) Cyclooxygenase and inflammation in Alzheimer's disease: experimental approaches and clinical interventions. J Neurosci Res 54:1–6.

Paxinos G, Franklin KBJ (2001) The mouse brain in stereotaxic coordinates, Ed 2. San Diego: Academic.

Paxinos G, Watson C (1998) The rat brain in stereotaxic coordinates, Ed 2. San Diego: Academic.

Piani D, Spranger M, Frei K, Schaggner A, Fontana A (1992) Macrophage-induced cytotoxicity of N-methyl-D-aspartate receptor positive neurons involves excitatory amino acids rather than oxygen intermediates and cytokines. Eur J Immunol 22:2429–2436.

Poltorak A, He X, Smirnova I, Liu MY, Van Huffel C, Du X, Birdwell D, Alejos E, Silva M, Galanos C, Freudenberg M, Ricciardi-Castagnoli P, Layton B, Beutler B (1998) Defective LPS signaling in C3H/HeJ and C57BL/10ScCr mice: mutations in Tlr4 gene. Science 282:2085–2088.

Roher AE, Weiss N, Kokjohn TA, Kuo YM, Kalback W, Anthony J, Watson D, Luehrs DC, Sue L, Walker D, Emmerling M, Goux W, Beach T (2002) Increased A beta peptides and reduced cholesterol and myelin proteins characterize white matter degeneration in Alzheimer's disease. Biochemistry 41:11080–11090.

Schipke CG, Ohlemeyer C, Matyash M, Nolte C, Kettenmann H, Kirchhoff F (2001) Astrocytes of the mouse neocortex express functional N-methyl-D-aspartate receptors. FASEB J 15:1270–1272.

Schmued LC, Albertson C, Slikker Jr W (1997) Fluoro-Jade: a novel fluorochrome for the sensitive and reliable histochemical localization of neuronal degeneration. Brain Res 751:37–46.

Simonian NA, Coyle JT (1996) A oxidative stress in neurodegenerative diseases. Annu Rev Pharmacol Toxicol 36:83–106.

Soulet D, Rivest S (2003) Polyamines play a critical role in the control of the innate immune response in the mouse central nervous system. J Cell Biol 162:257–268.

Stoll G, Jander S (1999) The role of microglia and macrophages in the pathophysiology of the CNS. Prog Neurobiol 58:233–247.

Szczepanik AM, Fishkin RJ, Rush DK, Wilmot CA (1996) Effects of chronic intrahippocampal infusion of lipolysaccharide in the rat. Neuroscience 70:57–65.

Toshchakov V, Jones BW, Perera PY, Thomas K, Cody MJ, Zhang S, Williams BR, Major J, Hamilton TA, Fenton MJ, Vogel SN (2002) TLR4, but not TLR2, mediates IFN-beta-induced STAT1alpha/beta-dependent gene expression in macrophages. Nat Immunol 3:392–398.

Underhill D, Ozinsky A (2002) Toll-like receptors: key mediators of microbe detection. Curr Opin Immunol 14:103–110.

Wallin RP, Lundqvist A, More SH, Bonin A, Kiessling R, Ljunggren HG (2002) Heat-shock proteins as activators of the innate immune system. Trends Immunol 23:130–135.

Werner P, Pitt D, Raine CS (2001) Multiple sclerosis: altered glutamate homeostasis in lesions correlates with oligodendrocyte and axonal damage. Ann Neurol 50:169–180.